*Geologie en Mijnbouw* **68**: 345–356, 1989.


# The relationship between deformation and metamorphism in the Canigou Massif, Pyrenees: a case study

R.L. Gibson
*Department of Earth Sciences, University of Cambridge, Cambridge, CB2 3EQ, U.K.*

Received 8 November 1988; accepted in revised form 15 March 1989

**Abstract**
Previous interpretations of the structure of the Canigou massif have related the development of the regional foliation to tectonic emplacement of the Canigou orthogneisses within the Infracaradocian sediments (Guitard 1970, Casas 1978, Lagarde 1978). Re-investigation of the structural evolution of the massif has shown that the regional foliation (S3) is preceded by the development of a pervasive S1 foliation and localized large-scale D2 folding. D2 folds affect the contact between the Canigou orthogneisses and underlying metasediments, indicating that the orthogneisses were emplaced within the sedimentary sequence prior to the development of the regional foliation. S3 is a subhorizontal crenulation foliation subparallel to S0-S1, except locally where D2 folding results in a more discordant relationship. Regional doming of S3 is associated with post-D3 folding and mylonite development. Porphyroblast-matrix microtextural relationships indicate that the peak of Hercynian low-P-high-T regional metamorphism is synchronous with progressive development of S3. Complex $S_i/S_e$ geometries indicate that deformation was inhomogeneous on a small scale.

## Introduction

The relation between deformation and metamorphism in regional metamorphic terranes provides important clues to the tectonic environment in which metamorphism occurred (e.g. Thompson & Ridley 1987). In the Hercynian low-P-high-T regional metamorphic terrane exposed in the Pyrenees, it is generally recognised that metamorphism is closely related to the development of a regional subhorizontal foliation. Various tectonic models have been proposed to explain this relationship and the origin of the subhorizontal foliation, among them diapiric doming (Soula 1982), crustal extension (Wickham & Oxburgh 1987, Van den Eeckhout 1986) and crustal-scale compression (Guitard 1970, Soula et al. 1986).

This paper examines the relationship between Hercynian metamorphism and deformation in the Canigou massif, Eastern Pyrenees. A brief description is given of the chronology of deformation events which affect the massif and of the regional distribution of the deformation structures. The timing of metamorphism with respect to deformation is elucidated by examination of porphyroblast-matrix microtextural relationships within metapelitic lithologies in the massif. Finally, the data presented here are compared with observations from other areas in the Pyrenees and the implications for Hercynian tectonics are discussed.

## The Canigou Massif

The Canigou massif forms the eastern part of the composite Canigou-Caranca massif within the Axial Zone of the Eastern Pyrenees (Fig. 1a). It displays a broad east-plunging antiformal structure and is bounded and cut by fault- and mylonite-zones. The deepest structural levels (in the west of

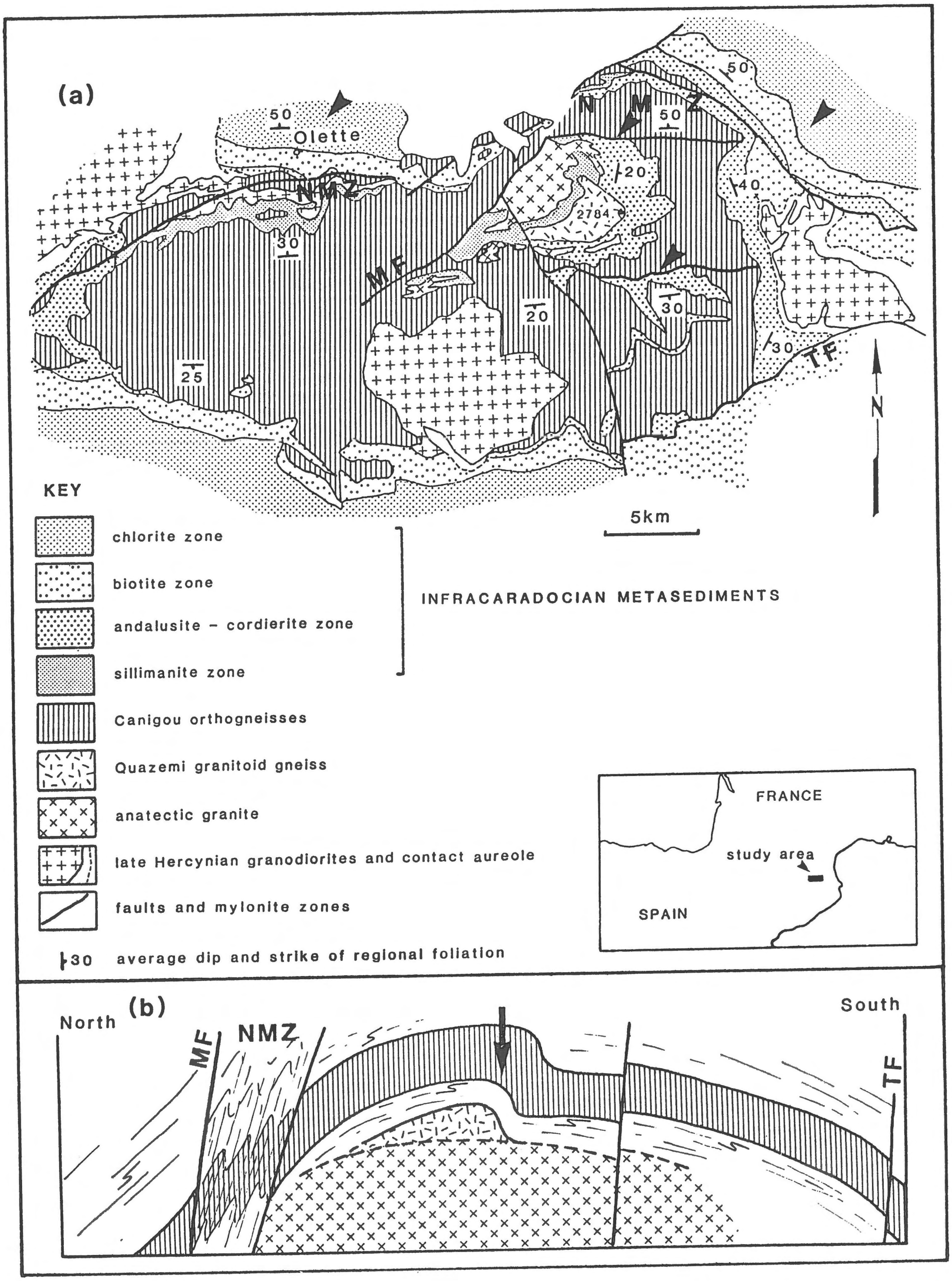


*Fig. 1.* (a) Geological map of the Canigou-Caranca massif, showing the metamorphic zones (modified, after Guitard, 1970). Arrows indicate the areas examined in the present study. NMZ – Northern Mylonite Zone; MF – Mantet-Fillols Fault; TF – Tech Fault. (b) Schematic N-S cross-section through the Canigou massif (not to scale) showing the vergence of $F_3^1$ folds. Note the subparallelism of S3 and the main lithological banding, except in the summit of the massif (arrowed). Abbreviations and key as for Fig. 1a (metasediments unornamented).

the massif adjacent to the Mantet-Fillols fault) correspond to the highest metamorphic grades and are dominated by an anatectic granite of Hercynian age which intrudes the suprajacent lithologies. Overlying this and intercalated within the metasedimentary succession is a sequence of orthogneisses, the Canigou gneisses (Guitard 1970), which have been interpreted as the granitoid basement upon which the Infracaradocian sediments were deposited (Guitard 1964, Vitrac-Michard & Allègre 1975a, 1975b). The intercalation of these gneisses within the sedimentary succession is thus believed to represent a nappe structure (Guitard 1964, 1970, Lagarde 1978, Casas 1978). These authors maintain that:

a) the regional foliation – S1 of Guitard 1970 and Lagarde 1978, S2 of Casas 1978, S3 of Laumonier & Guitard 1978 – is the product of this nappe-forming event, and
b) prograde metamorphism developed during – and peaked after – the development of this foliation, with porphyroblast growth being mimetic on these structures (Guitard 1970).

Four main areas, constituting some 120 km$^2$, were chosen in different parts of the massif (see Fig. 1a) in order to establish a chronology of deformation events and to examine the areal distribution of the regional foliation. Over 150 samples of metapelitic lithologies were sectioned to analyse the microstructures associated with this foliation and the relationship between these structures and porphyroblast phases.

**Deformation history**

Three main phases of deformation have been recognised in the massif preceding the development of retrogressive mylonitic structures.

A pervasive foliation (S1) subparallel to – and locally transposing – lithological layering (S0) and axial planar to small-scale tight to rootless isoclinal folds, provides evidence of the earliest deformation (D1) seen in the massif. Vergence directions for these folds are difficult to determine but fold axes are parallel to an intersection lineation ($L_1^0$, terminolgy after Bell & Duncan 1978) with a general NNE–SSW to NE–SW trend. (Henceforth in this paper 'S1' is used to denote the composite S0–S1 foliation).

A large-scale, SSE-verging antiform-synform pair, with upright to steeply inclined (north-dipping) axial planes, folds S1 in the summit of the massif (Fig. 1b). This is D2. The folds plunge shallowly to the ENE (Gibson, unpublished data) and have a wavelength and amplitude of at least several hundred metres. An axial planar S2 foliation is found only locally within the hinge zone of the antiform. Small-scale D1 structures are best seen on the steep S-dipping limb of this fold. Laumonier & Guitard (1978) report large-scale D2 folds in metasediments to the west of Olette (Fig. 1a).

D3 is responsible for the development of the regional foliation (S3) and intersection lineation ($L_3^1$) in the massif. In the lower metasediments it comprises a pervasive mm- to cm-scale subhorizontal crenulation foliation, S3, which is the dominant structure in the meta-pelitic lithologies. In most of the area S3 is subparallel to the large-scale lithological banding, with the exception of the steep F2 fold limb. Here D3 is a poorly developed subhorizontal crenulation foliation at a high angle to this banding.

In the chlorite zone north of Olette (Fig. 1a) S3 forms an axial plane crenulation cleavage associated with dm- to m-scale folds of S1 and lithological layering. D3 microstructures are developed heterogeneously around such folds. This relationship is represented schematically in Fig. 2a. The folds are generally asymmetric, with the microstructure in the long limbs (A in Fig. 2a) being dominated by a strong, planar S3 cleavage which is subparallel to S1. Evidence of $F_3^1$ microfolds here is rare. Within the fold hinges and median limbs (B and C respectively in Fig. 2a) the microstructure is dominated by microfolds of S1 with a spaced S3 cleavage developed on microfold limbs.

In the biotite zone here and in the east of the massif (Fig. 1a) the greater degree of recrystallisation and growth of phyllosilicates obscures the lithological layering. No direct evidence is thus found of these larger-scale $F_3^1$ folds, but microtextural domains dominated by planar fabrics and others dominated by microfolded S1 with limited S3 development are found within the same outcrop. Por-

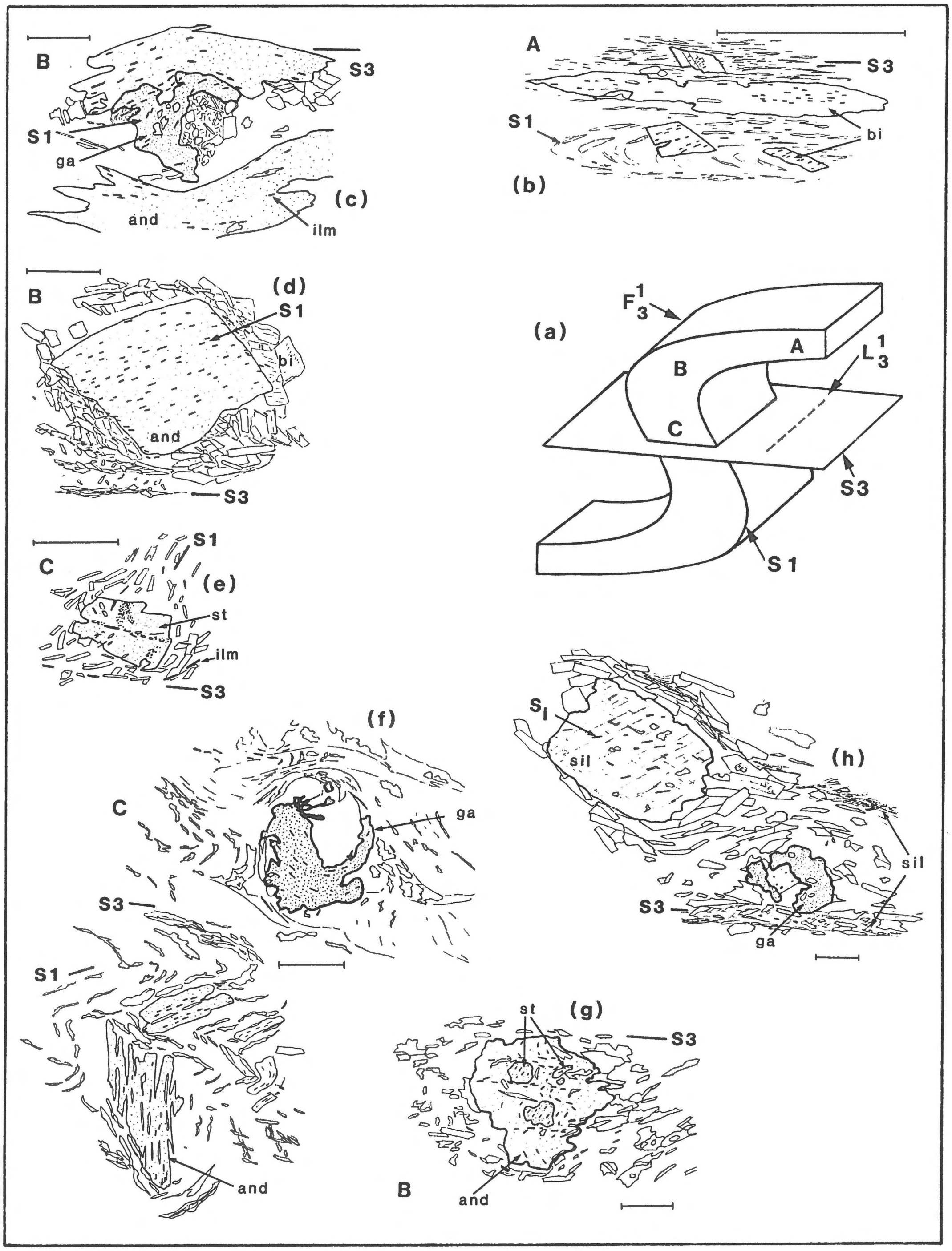


*Fig. 2.* Variable porphyroblast-matrix microtextural relationships interpreted as the product of heterogeneous development of S3 associated with larger-scale $F_3^1$ folds. A, B and C indicate the inferred position of each section with respect to the larger-scale fold (Fig. 2a). All sections are normal to $L_3^1$. Scale bars equal 1 mm. b) Biotite (bi) preferentially elongated parallel to S3 and with deflection of $S_e$ with respect to $S_i$. c) Garnet (ga) overgrowing $F_3^1$. S3 is deflected around the garnet and overgrown by andalusite (and). d) Type 3 andalusite. $S3_e$ is well defined (see text for explanation). e) Type 2 staurolite (st; see text for explanation). f) Snowball garnet and Type 3 andalusite. g) Type 2 andalusite overgrowing Type 3 staurolite relics. S3 is more strongly developed in the matrix. h) Intense S3 foliation defined by biotite and sillimanite. S3 is deflected around corroded garnet and sillimanite (si) pseudomorphs of andalusite. Note planar $S_i$ in sillimanite. Specimen location: b) biotite zone; c), d) and e) andalusite-cordierite zone, upper metasediments (staurolite stable); f) and g) andalusite-cordierite zone, lower metasediments (staurolite unstable); h) sillimanite zone, lower metasediments.

phyroblast inclusion trails similarly suggest that such folds did exist in the higher grade zones at some time during D3 (see below).

Within the lower metasediments, $F_3^1$ folds verge consistently in a general northwesterly direction with a shallowly-plunging $L_3^1$ lineation oriented NE–SW to ENE–WSW. S3 dips shallowly to the S in the south and to the NE in the north. In the upper metasediments in the east of the massif, S3 is reoriented by younger upright folds which are locally associated with subvertical retrogressive mylonite zones. Evidence of $F_3^1$ vergence is more difficult to obtain, but appears to be generally northwestward to northward. In the Olette region S3 dips moderately steeply to the NNE. Detailed studies here by Laumonier & Guitard (1978) have shown a general northwestward vergence for $F_3^1$ (their $F_d$). These authors note that the presence of large-scale D2 folds, which reorientate S1, results in variation in the angle between S1 and S3, and hence in the vergence of $F_3^1$ and in the orientation of the D3 intersection lineation.

It is thus apparent that D3 structures are consistent throughout the areas examined, despite changes in orientation of S3. The variable S3 orientation in the massif is regarded as the product of post-D3 deformation. Guitard (1970) relates this antiformal shape to the interference of two fold sets postdating formation of the regional foliation and oriented NE–SW and ESE–WNW respectively. Carreras et al. (1980) and Casas (1984) maintain that the domal aspect of the massif is the product of folding and associated mylonitic deformation postdating the setting of the Hercynian metamorphic isograds and the development of the regional foliation. These mylonites also affect the late Hercynian granodiorite intrusions.

## Metamorphism

Metamorphic grade increases with structural depth, attaining a maximum in the west of the massif. Isograds are broadly parallel to the major lithological units (Guitard 1970), but mylonite and fault zones postdating the setting of the isograd sequence hamper more accurate geometrical information being obtained from them. Fig. 1a shows the distribution of the main isograds, mapped in detail by Guitard (1970). Staurolite first appears within the andalusite-cordierite zone in the upper metasediments but becomes unstable above the contact with the Canigou orthogneisses. Garnet first appears in the lower biotite zone (Guitard 1970) and persists through all subsequent grades both as a stable phase and as unstable relics.

The metamorphism is progressive, as is seen by the preservation of relict staurolite in andalusite in the lower andalusite-cordierite zone, the development of sillimanite pseudomorphs after andalusite zone, and garnet zoning profiles. Metamorphism culminated in partial melting of metasediments to give rise to the anatectic granite. This was mobilised and intruded the lower metasediments, both as semi-concordant leucogranite veins which are boudinaged parallel to S3 and as pegmatite dykes which cross-cut S3. Coarse muscovite associated with these dykes overgrows S3 and peak metamorphic porphyroblast phases.

## Relationship between metamorphism and deformation

### *The S3 foliation*

The nature of the S3 foliation varies as a function of metamorphic grade. In the chlorite zone it is a discrete or zonal cleavage (Gray 1979) defined by graphite, iron hydroxides, phengitic mica and chlorite. In the biotite zone, increasing recrystallisation and growth of phyllosilicates produces a differentiated crenulation schistosity defined by phyllosilicate-rich domains (predominantly white mica, with chlorite, biotite, graphite and some opaques) and quartz-rich domains, although the discrete cleavage does persist in places.

Within the andalusite-cordierite zone, chlorite decreases in abundance and S1 and S3 are defined by ilmenite, graphite, white mica and biotite laths. Biotite, in particular, is coarser. Below the staurolite-out isograd, in the lower metasediments, S3 is most often defined by biotite lamellae in which biotite (001) displays a crude maximum parallel to S3. $F_3^1$ microfolds are defined by finer-grained mica and ilmenite in quartz-rich layers and by polygonal arcs of muscovite in mica-rich layers. The coarse grain size of the phyllosilicates and the presence of porphyroblasts here obscures the fine-scale layering seen in the chlorite zone. In the sillimanite zone this layering is further obliterated by the segregation of quartz-feldspar leucosomes and development of sillimanite-biotite mats parallel to S3. Only rare $F_3^1$ microfolds, defined by sillimanite aggregates, provide evidence of the crenulation origin of S3.

*Relationships between porphyroblasts and S3*

The relationships between porphyroblasts and matrix, and particularly those between the inclusion trails within the porphyroblasts ($S_i$) and the adjacent matrix foliation ($S_e$) within regionally metamorphed lithologies, provide evidence of the timing of porphyroblast growth with respect to deformation (e.g. Zwart 1962, Vernon 1978, Bell & Rubenach 1983). Porphyroblast-bearing meta-pelitic lithologies from the Canigou massif have been examined microscopically to elucidate the relationship between metamorphism and D3. The observed relationships between porphyroblasts and matrix structures are summarized in Figs 2 and 3. Unless otherwise stated, all sections are cut perpendicular to $L_3^1$.

*Biotite* porphyroblasts in the lower biotite zone and upper andalusite-cordierite zone display preferential elongation parallel to S3 (Fig. 2b). They are commonly strained, and pressure shadows of white mica and fine-grained biotite may occur adjacent to them (Fig. 3a). Slight angular discordances of up to 25° between $S_i$ and $S_e$ are common but the sense of deflection of $S_i$ with respect to $S_e$ is not consistent within individual samples. In view of the strain-shadows developed adjacent to the porphyroblasts it is tempting to suggest that they rotated in opposite directions during progressive bulk shortening in a manner similar to models proposed by Zwart (1962) and Lister et al. (1986). Examination of samples preserving $F_3^1$ microfolds, however, shows that the porphyroblasts overgrow both S3 and the microfolds of S1. Where they overgrow the latter the $S_i$ trails are oblique $S3_e$. Subsequent post-porphyroblast D3 deformation has rotated S1 outside the porphyroblasts into parallelism with $S3_e$ whilst the porphyroblasts maintained their original orientation (see Ramsay 1962, Vernon 1988). The lower the angle between S1 and S3 when the biotite grew, the smaller the discrepancy between $S_i$ and $S_e$. Similarly, if S3 rotated progressively in response to a changing local strain ellipsoid (see Ramsay 1962, Williams 1977), non-rotating biotite porphyroblasts overgrowing an early stage of S3 would preserve an orientation oblique to the final matrix orientation of S3. Within the lower metasediments similar biotite-matrix relationships are seen in mica-rich layers and within andalusite porphyroblasts.

*Chlorite* porphyroblasts display $S_i$ geometries of folded S1 and of $S3_i$ oblique to $S3_e$, similar to those described above.

*Staurolite* in the staurolite zone displays 3 types of $S_i$ geometries in sections normal to $L_3^1$. As with biotite, $S_i$ is continuous with $S_e$ which is deflected around the staurolite. In sections parallel to $L_3^1$, porphyroblasts are occasionally boudinaged, with development of muscovite in the boudin necks.

Type 1 staurolite occurs in lithologies with strong S3 development. Porphyroblasts contain planar $S_i$ trails continuous with – but slightly oblique to – $S3_e$. Staurolite overgrew S3 and/or S1 which was subparallel to S3, after which $S_e$ was rotated to its present configuration by continuing D3 deformation. Type 2 staurolite (Fig. 2e) occurs where folding of S1 (and therefore development of S3) is less intense. It contains curved S1 trails and planar S3 trails. Types 1 and 2 have been found together in individual specimens. Type 3 staurolite contains planar inclusion trails parallel to S1. In Fig. 3b these are continuous with folded S1 trails in the matrix which is in turn characterised by a well-defined S3 foliation. In the lower metasediments, where staurolite is unstable and is only found as relics within andalusite, the porphyroblasts contain planar $S_i$ which ranges from subparallel to perpendicular to $S3_e$ (Fig. 2g).

*Garnet* in the andalusite-cordierite and sillimanite zones displays a variety of internal inclusion geometries. Snowball garnets (Figs 2f and 3c) show variable rotation in excess of 180°. (This is a minimum estimate based upon the observation that $S_i$ within the core of the garnet is likely to be S1, with an angular relationship unknown with respect to S3 at the time of commencement of garnet growth.) The outer parts of the garnet show typical features described by Schoneveld (1977), notably intersecting ilmenite and quartz helixes and continuity between quartz helixes and pressure-shadow regions in the adjacent matrix.

Garnet with sigmoidal inclusion trails also indicates syn-D3 crystallisation, overgrowing $F_3^1$ microfolds (Fig. 2c) yet being wrapped by – and commonly preferentially resorbed adjacent to – $S3_e$ (Fig. 3d). Boudinage and fracturing of porphyroblasts is also found.

In muscovite-rich lithologies in the lower metasediments garnet may be totally pseudomorphed by biotite +/− muscovite aggregates which preserve the outline of the original crystal around which S3 is wrapped. Andalusite encloses similarly pseudomorphed garnet in the same rocks. In the upper metasediments garnet, like staurolite, is found enclosed within, but in textural equilibrium with, andalusite. In one sample staurolite partially encloses garnet but this is insufficient evidence for defining relative timing of the respective porphyroblast phases. Further definitive textural evidence is lacking.

*Andalusite* is the most ubiquitous porphyroblast phase in the massif. Porphyroblasts display similar microtextural relationships to staurolite:
Type 1 andalusite contains planar $S_i$. It occurs where S3 is strongly developed in the matrix and S1 and S3 are indistinguishable from one-another. $S3_e$ and $S_i$ are continuous but may be slightly oblique. In sections parallel to $L_3^1$, porphyroblasts may be boudinaged, with growth of muscovite and quartz in the boudin necks. In Fig. 2c andalusite overgrows S3 which is deflected around a garnet porphyroblast. Type 2 andalusite contains S3 and crenulated S1 trails (Fig. 3e). This is the most common form of inclusion geometry, particularly in the lower metasediments (Fig. 2g). In all cases $S3_e$ is deflected around the andalusite and $F_3^1$ crenulations in the matrix are tighter. Type 3 andalusite contains S1 trails, either planar (Fig. 2d and f) or curved (Fig. 3f). $S_i$ is commonly at a high angle to $S_e$, but is strongly deflected into continuity with $S_e$ near the porphyroblast margins (Fig. 2d).

In the sillimanite zone *sillimanite* pseudomorphs andalusite which contains planar $S_i$ oblique to S3 and which is strongly deflected into parallelism with $S3_e$ adjacent to porphyroblasts. No evidence of strong $S3_i$ fabrics has been found in the porphyroblasts at this level of the massif. Sillimanite also occurs as fibrous aggregates intergrown with biotite parallel to $S3_e$, and defining rare isoclinal crenulation hinges.

*Cordierite* is rarely found as unaltered crystals. It occurs as rounded porphyroblasts and displays similar textures to andalusite in the andalusite-cordierite zone. In the sillimanite zone cordierite occurs adjacent to embayed garnet and overgrows fibrolite oriented parallel to S3.

*Interpretation*

Previous workers in the Canigou massif have interpreted porphyroblast-matrix microtextural relations, with exception of snowball garnets, as indicative of post-tectonic growth (Guitard 1970, Casas 1978). The evidence presented above, however, indicates syn-tectonic growth. Among these features are:

1. Snowball garnets (Fig. 3c);
2. Garnet with sigmoidal $S_i$ continuous with $S_e$ (Fig. 2c);
3. Garnet which has overgrown $F_3^1$ microfolds being preferentially resorbed on surfaces adjacent to the S3 foliation such that $S_i$ is truncated (Fig. 3d);
4. Continuity between $S_i$ and $S_e$ with progressive deflection of $S_i$ towards the edge of the porphyroblast (Figs 2d and 3f);
5. $S_i$ geometries show a consistently less-evolved stage in the evolution of the S3 foliation than is present in the adjacent matrix (Figs 2d and 3e);
6. Boudinage of prophyroblasts;
7. Wrapping of the $S3_e$ foliation around porphyroblasts containing $F_3^1$ microfold trails or even $S3_i$ (Fig. 3e).

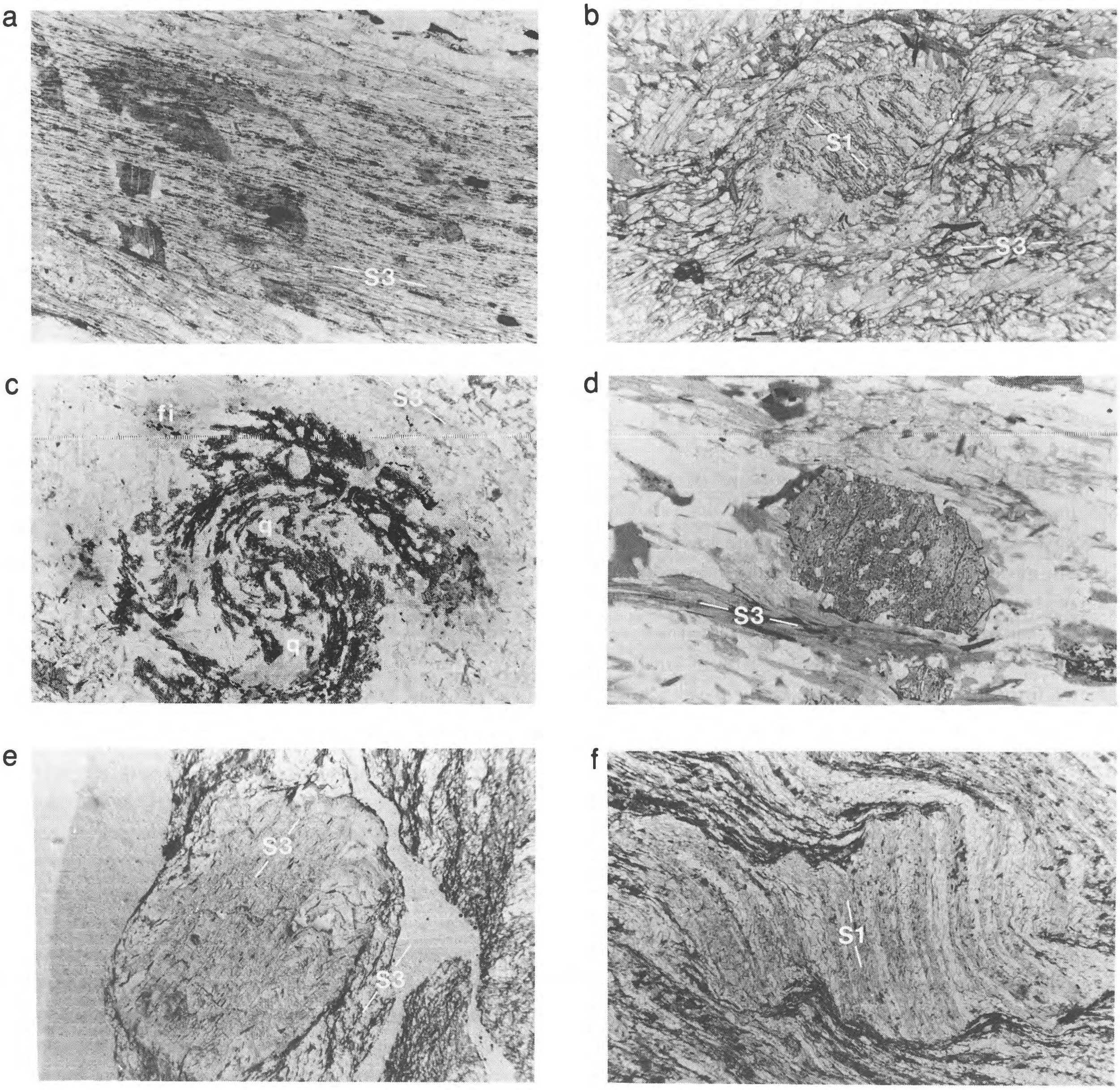


*Fig. 3.* Porphyroblast-matrix relationships. A, B and C refer to Fig. 2a. a) biotite (A). Note pressure shadows (centre, left), preferential elongation parallel to S3, and deflection of $S_i$ and $S_e$. b) Type 3 staurolite (B). Ilmenite inclusions defining S1 in the matrix are crenulated. c) Skeletal snowball garnet indicating top-to-the-left sense of shear (B). (q = quartz helix; fi = fibrolite). d) Garnet containing $F_3^1$ folds preferentially dissolved adjacent to S3 (B). e) Type 2 andalusite (B). f) Type 3 andalusite (C). The porphyroblast contains strongly deflected $S_i$ trails at its margins. (Length of field of view: a: 2.8 mm; b: 6.2 mm; c: 5.8 mm; d: 3.1 mm; e: 8 mm; f: 10 mm.)

From this evidence, the peak of Hercynian metamorphism in the massif is regarded as having occurred during the progressive D3 deformation.

One of the most striking results of this study is that, within a single thin section, a variety of microtextural relationships can exist between porphyroblasts and matrix and, within an individual outcrop, it is possible to find all types of $S_i/S_e$ geometries developed for a particular mineral. Three possible causes for such variation should be considered:

1. Metamorphism is progressive and the isotherm corresponding to a particular porphyroblast-producing reaction migrates at a slower rate than that at which deformation occurs. Thus, as the isotherm migrates through the rock pile, porphyroblasts will be produced at successively later stages of D3. Porphyroblasts at successively lower metamorphic grades should thus contain more evolved stages of S3 development.
2. Metamorphism is progressive and porphyroblasts develop by continuous reactions. Bulk rock composition will thus play a role in determining the temperature (and, hence, the time) at which porphyroblasts will develop with respect to D3.
3. Deformation is inhomogeneous, in which case porphyroblasts growing at the same time in a rock mass will overgrow different structures as a result of variation in intensity and type of strain within the rock (deformation partitioning).

The heterogeneous structures observed within an individual porphyroblast species occur on the scale of individual thin sections in rocks with an homogeneous bulk composition (e.g. Figs 2c and 3e). Furthermore, the porphyroblasts themselves show no change in composition within an individual specimen, despite their variable $S_i$ geometries (Gibson, unpublished data), indicating that they formed by the same reaction. This, and the evidence of heterogeneous development of S3 as a result of outcrop-scale (and smaller) $F_3^1$ folds indicates that complex porphyroblast-matrix microtextural relationships observed in the massif are the product of inhomogeneous D3 deformation. It also shows that porphyroblasts containing planar S1 inclusion trails (e.g. Type 3 staurolite) have grown syn-tectonically, because porphyroblasts in the same rock, produced by the same reaction, overgrow $F_3^1$ microfolds and S3, and are thus obviously syn-D3.

Where such heterogeneity within individual specimens does not exist, as occurs with staurolite in the lower metasediments and pseudomorphed andalusite in the sillimanite zone, the possibility that the porphyroblasts grew prior to D3 should not be discounted. Conversely, it has been shown above that the presence of a planar $S_i$ which is oblique to $S_e$ does not constitute unequivocal proof of a pre-tectonic origin for the porphyroblast (e.g. Fig. 2b).

Finally, microtextural studies provide corroborative evidence of the prograde metamorphic reactions in the massif. The preservation of planar $S_i$ within staurolite which is being replaced by andalusite which overgrows both $F_3^1$ microfolds and S3 indicates that staurolite grew prior to the development of the microfolds and that it broke down after the formation of such features in the adjacent matrix (Fig. 2g). Similarly, garnet which overgrows $F_3^1$ microfolds is undergoing prograde breakdown (in the presence of muscovite) to biotite + andalusite + quartz + ilmenite preferentially on surfaces parallel to S3 (Fig. 3d). The resultant andalusite overgrows S3.

## Discussion and conclusions

The development of the subhorizontal regional foliation in the Canigou massif has previously been considered to be related to tectonic emplacement within the Infracaradocian sediments of the Canigou gneisses as the core of a large-scale nappe structure (Guitard 1970, Casas 1978, Lagarde 1978). Analysis of the structure of the summit of the massif has shown that this foliation is a D3 structure and that it is preceded by a phase of upright folding (D2) which deforms the contact between the Canigou gneisses and the lower metasediments. The Canigou gneisses were thus intercalated within the sedimentary sequence prior to the development of the regional foliation. It is not apparent whether emplacement of the gneisses is of igneous origin, such as has been suggested by Jäger & Zwart (1968) for the Aston-Hospitalet gneisses, or of tectonic origin (possibly during D1). The most important conclusion which can be drawn from this is that the Hercynian low-P-high-T metamorphism here is not associated with nappe tectonics, as maintained by Guitard (1970).

In the Canigou massif the S3 foliation displays a domed aspect. Workers here, however, attribute this to the effects of post-D3 folding and mylonite development on an initially planar foliation (Guitard 1970, Carreras et al. 1980, Casas 1984, Gibson unpublished data). Furthermore, if doming occurred during D3, then $F_3^1$ folds should show opposite senses of vergence on opposite sides of the dome. This does not appear to be the case in the massif. These folds show a broadly consistent vergence to the NW in all structural levels of the massif, with the exception of localized areas where large-scale pre-D3 folding has reoriented S0–S1 (Laumonier & Guitard 1978, Fig. 1b). This consistency of vergence, and the apparent lack of large-scale D3 fold structures is more compatible with non-coaxial deformation such as is found within a ductile shear zone. Geometrical relationships indicate a top-to-the-NW sense of displacement.

Any tectonic mechanism which is invoked to explain the development of the S3 foliation must also take into consideration the metamorphic history of the massif. Various models have been proposed to explain the close relationship between Hercynian metamorphism and the formation of the regional foliation in other massifs in the Pyrenees. Among them are:

1. Diapiric rise of granitoid bodies, with the regional foliation forming as a result of subvertical flattening. Deformation is regarded as occurring as a single, progressive event (Soula 1982, De Bresser et al. 1986) or as more than one discrete event (Verhoef et al. 1984). Doming of the regional foliation and the isograds occurs during their development, not afterwards.
2. Non-coaxial deformation in a crustal-scale extensional ductile shear zone (Van den Eeckhout 1986, Van den Eeckhout & Zwart 1988). These authors recognize that, whilst this model may explain the development of the regional foliation, it cannot account for the large heat input required to effect the andalusite-sillimanite transformation during prograde low-P-high-T regional metamorphism (see also England & Thompson 1984, Thompson & Ridley 1987).
3. Crustal-scale extension and intrusion of mafic magma into the lower crust (Wickham & Oxburgh 1987). The intrusion provides the heat for regional metamorphism.

Evidence from the Canigou massif, presented above, agrees well with the model of an extensional shear zone (Van den Eeckhout & Zwart 1988). Numerical modelling by McKenzie & Bickle (1988) predicts that lithospheric extension will generate significant amounts of melt in the upper mantle. The importance of this model is that extension causes the generation of hot mafic or ultramafic melts, the upward movement of which could produce the necessary heat input into the crust for low-P-high-T regional metamorphic to proceed.

In order to evaluate and refine the existing tectonothermal models proposed for the Hercynian Pyrenees, it is necessary to establish a clear relationship between the metamorphic evolution and the tectonic history of the terrane. Establishing unambiguous relationships between the growth of metamorphic mineral assemblages and the deformation structures is the most effective way of doing this. The present study has shown that complex porphyroblast-matrix microtextural relationships in the Canigou massif provide unequivocal evidence of syn-tectonic porphyroblast growth during progressive, inhomogeneous deformation. Elsewhere in the Pyrenees porphyroblast-matrix microtextural relationships have been interpreted as indicative of the peak of metamorphism postdating the development of the regional foliation (e.g. Zwart 1979, Verhoef et al. 1984, De Bresser et al. 1986, Soula et al. 1986, Van den Eeckhout 1986, Wickham & Oxburgh 1987). In all cases porphyroblast growth is interpreted as having commenced during and, occasionally, even prior to, foliation development. Zwart (1979) represents the peak of metamorphism as diachronous with respect to deformation, being later at higher metamorphic grades than at lower grades. Soula et al. (1986) maintain that it is earlier at higher grades.

This investigation has touched upon one of the most crucial aspects of the study of regionally metamorphosed terranes. In order to elucidate the tectonothermal history of a metamorphic belt, it is essential to understand how the processes of progressive metamorphism and progressive, inhomogeneous deformation interact. The low-P-high-T metamorphic terrane exposed in the Pyrenees presents an opportunity to examine the spatial and temporal relationships between regional-scale metamorphism and deformation and from this to construct an evolutionary model for the crust here during Hercynian times.

## Acknowledgements

I am indebted to Mike Bickle, Bobby John, Ioan Jones and Dave Large for discussion of early drafts of this manuscript, and Folkert Majoor and an anonymous reviewer for their comments. Financial support from the Cambridge Livingstone Trust, the Victoria League Trust and the Hepburn, Ballot and Wahl Trusts is gratefully acknowledged. Earth Sciences Contribution No. 1355.

## References

Bell, T.H. & Duncan, A.C. 1978 A rationalized and unified shorthand terminology for lineations and fold axes in tectonites – Tectonophysics 47: T1–T5

Bell, T.H. & Rubenach, M.J. 1983 Sequential porphyroblast growth and crenulation cleavage development during progressive deformation – Tectonophysics 92: 171–194

Carreras, J., Julivert, M. & Santanach, P. 1980 Hercynian mylonite belts in the eastern Pyrenees: an example of shear zones associated with late folding – J. Struct. Geol. 2: 5–9

Casas, J.M. 1978 Estudi de les primeres fases de deformacio hercinianes a la 'Finestra Tectonica de Balaig'. Massis del Canigo – Tesi Llicenc., Univ. Barcelona: 112 pp

Casas, J.M. 1984 Estudi de la deformacio en els gneiss del massis del Canigou – Unpubl. Ph.D. Thesis, Univ. Barcelona: 284 pp

De Bresser, J.H.P, Majoor, F.J.M. & Ploegsma, M. 1986 New insights in the structural and metamorphic history of the western Lys-Caillauas massif (Central Pyrenees, France) – Geol. Mijnbouw 65: 177–187

England, P.C. & Thompson, A.B. 1984 Pressure-temperature-time paths of regional metamorphism. I. Heat transfer during the evolution of regions of thickened continental crust – J. Petrol. 25: 894–928

Gray, D.R. 1979 Microstructure of crenulation cleavages: an indicator of cleavage origin – Am. J. Sci. 279: 97–128

Guitard, G. 1964 Un exemple de structure en nappe de style pennique dans la chaine hercynienne: les gneiss stratoides du Canigou (Pyrenees-Orientales) – C.R. Acas. Sc. 258: 4597–4599

Guitard, G. 1970 Le métamorphisme hercynien mesozonal et les gneiss oeillés du massif du Canigou (Pyrénées Orientales) – Fr. Bur. Rech. Géol. Minieres Mem: 317 pp

Jäger, E. & Zwart, H.J. 1968 Rb-Sr Age determinations of some gneisses and granites of the Aston-Hospitalet massif (Pyrenees) – Geol. Mijnbouw 47: 349–357

Lagarde, J.L. 1978 La déformation des roches dans les domaines à schistosite subhorizontale – Thèse 3ème cycle, Univ. Rennes: 164 pp

Laumonier, B. & Guitard, G. 1978 Contribution à l'étude de la tectonique superposée hercynienne des Pyrénées Orientales: le problème des plissements précoces dans le Paléozoique inférieur épizonal (Série de Jujols) du Synclinal de Villefranche de Conflent – Rev. Geogr. Phys. Géol. Dyn. (2), 20: 177–212

Lister, G.S., Boland, J.N. & Zwart, H.J. 1986 Step-wise growth of biotite porphyroblasts in pelitic schists of the western Lys-Caillauas massif (Pyrenees) – J. Struct. Geol. 8: 543–562

McKenzie, D. & Bickle, M.J. 1988 The volume and composition of melt generated by extension of the lithosphere – J. Petrol. 29: 625–680

Ramsay J.G. 1962 The geometry and mechanics of formation of 'similar' type folds – J. Geol. 70: 309–327

Schoneveld, C. 1977 A study of some typical inclusion patterns in strongly paracrystalline-rotated garnets – Tectonophysics 39: 453–471

Soula, J.C. 1982 Characteristics and mode of emplacement of gneiss domes and plutonic domes in central-eastern Pyrenees – J. Struct. Geol. 4: 313–342

Soula, J.C., Debat, P., Deramond, J. & Pouget, P. 1986 A dynamic model of the structural evolution of the Hercynian Pyrenees – Tectonophysics 129: 29–51

Thompson, A.B. & Ridley, J.R. 1987 Pressure-temperature-time (P-T-t) histories of orogenic belts – R. Soc. Lond. Philos. Trans. Ser. A 321: 27–45

Van den Eeckhout, B. 1986 A case study of a mantled gneiss antiform, the Hospitalet Massif, Pyrenees (Andorra, France) – Geologica Ultraiectina 45: 193 pp

Van den Eeckhout, B. & Zwart, H.J. 1988 Hercynian crustal-scale extensional shear zone in the Pyrenees – Geology 16: 135–138

Verhoef, P.N.W., Vissers, R.L.M. & Zwart, H.J. 1984 A new interpretation of the structural and metamorphic history of the Western Aston Massif (Central Pyrenees, France) – Geol. Mijnbouw 63: 399–410

Vernon, R.H. 1978 Porphyroblast-matrix microstructural relationships in deformed metamorphic rocks – Geol. Rundsch. 67: 288–305

Vernon, R.H. 1988 Microstructural evidence of rotation and non-rotation of mica porphyroblasts – J. Metam. Geol. 6: 595–601

Vitrac-Michard, A. & Allègre, C.J. 1975a A study of the formation and history of a piece of continental crust by the $^{87}Rb$-$^{87}Sr$ method: The case of the French Oriental Pyrenees – Contrib. Mineral. Petrol 50: 257–285

Vitrac-Michard, A. & Allègre, C.J. 1975b $^{238}U$-$^{206}Pb$, $^{235}U$-$^{207}Pb$ systematics on Pyrenean basement – Contrib. Mineral. Petrol. 51: 205–212

Wickham, S.M. & Oxburgh, E.R. 1987 Low-pressure regional metamorphism in the Pyrenees and its implications for the thermal evolution of rifted continental crust – R. Soc. Lond. Philos. Trans. Ser. A 321: 219–242

Williams, P.F. 1977 Foliation: a review and discussion – Tectonophysics 39: 305–328

Zwart, H.J. 1962 On the determination of polymetamorphic mineral associations, and its application to the Bosost area (Central Pyrenees) – Geol. Rundsch. 52: 38–65

Zwart, H.J. 1979 The geology of the Central Pyrenees – Leidse Geol. Meded. 50: 74 pp